Raman Study of Mechanically Induced Oxygenation State Transition of Red Blood Cells Using Optical Tweezers

Satish Rao,[†] Štefan Bálint,[†¶] Benjamin Cossins,[‡] Victor Guallar,[§] and Dmitri Petrov[§*]

[†]ICFO-Institut de Ciències Fotòniques, [‡]Barcelona Supercomputing Center, and [§]Institucio Catalana de Recerca i Estudis Avancats, Barcelona, Spain; and [¶]Department of Biophysics, University of Pavol Jozef Šafárik, Košice, Slovak Republic

ABSTRACT   Raman spectroscopy was used to monitor changes in the oxygenation state of human red blood cells while they were placed under mechanical stress with the use of optical tweezers. The applied force is intended to simulate the stretching and compression that cells experience as they pass through vessels and smaller capillaries. In this work, spectroscopic evidence of a transition between the oxygenation and deoxygenation states, which is induced by stretching the cell with optical tweezers, is presented. The transition is due to enhanced hemoglobin-membrane and hemoglobin neighbor-neighbor interactions, and the latter was further studied by modeling the electrostatic binding of two of the protein structures.

INTRODUCTION

In a biological system, proteins, enzymes, and other molecular structures function with a delicate balance between small mechanical forces and chemical reactions. Some common and well-known examples are the stretching and twisting of DNA during its protein binding processes, and the protein conformational changes that occur along with biochemical processes.

For the latter case, hemoglobin (Hb) is a classical example of a protein that undergoes conformational or domain changes upon experiencing a chemical reaction—in this case, ligand binding. Hb, the main component of the cytoplasm of the red blood cell (RBC), is a globular protein that facilitates oxygen transport via binding to heme groups. Oxygen binding is a cooperative effect: the affinity increases due to stress-relieving conformational changes in the protein as a result of successive ligand binding. The protein is generalized by a two-state model between two alternate structures: 1), a deoxygenated (deoxy), low-affinity, tense (T) structure; and 2), an oxygenated (oxy), high-affinity, relaxed (R) structure (1). The connection between chemical binding and conformational change has led to the idea of using an external force to affect the oxygenation of the Hb (2).

There are two requirements to perform such an experiment. First, a tool is needed to isolate a cell and apply forces. Second, a method is necessary to monitor the chemical changes of the Hb under such a stress. Optical tweezers have become an established tool to accomplish the first task (3,4). With the use of a multibeam trap, a cell can be isolated and manipulated in a number of ways (5,6). The trapping system can then be coupled to a monitoring method, such as Raman spectroscopy (7). Raman spectroscopy has proved to be an important characterization tool for biological systems. The Raman fingerprint of a biological cell can yield a vast amount of information about the cell's structural makeup (8) and chemical changes (9), and can even be used as a form of cell identification (10) or imaging (11). In the basic configuration of the combined Raman tweezers system, a beam is used to trap a cell while the same or another beam simultaneously excites its Raman spectrum. The cell is thus isolated and can be studied without the effects of neighbor interactions. The typical powers and wavelengths for trapping and Raman excitation of living cells are below the lower limits of cell heating and photodegradation (12), as further exemplified by demonstrations of the proliferation of a cell in an optical trap (3,13).

From a Raman perspective, the RBC is an interesting system because of its relatively basic structure, and, although these cells offer a dense vibrational spectrum, the frequency regions have been well characterized (14,15). Studies focused on the oxygenation of the RBC have consistently revealed differences in spectrum between the oxy and deoxy states (14–17). There is general agreement regarding the assignment of certain bands as "oxygenation markers", i.e., Raman peaks that change in intensity and/or frequency based on the oxygenation state of the RBC.

A number of studies have used optical tweezers to apply force to biological systems to study their general properties or reactions (4,18). Included in these efforts have been many studies of the mechanical properties of RBCs. The unique deformability of these cells allows them to pass through small capillaries and slits in organs, often with diameters half the size of the cell. Studies of the mechanical structure of the membrane have related it to polymer physics (19). Mechanical force measurements have led to elasticity estimations (20–23), and stretching measurements have been used to distinguish between healthy and sick cells (22,24). The idea of a relation between RBC oxygenation and mechanical force has been discussed in some studies in reference to enhanced transport across a deformed permeable membrane (25) and the possibility of increased kinetics in

*Correspondence: dmitri.petrov@icfo.es

Editor: Brian R. Dyer.

the Hb (2). However, thus far there has been no direct measurement of this relation.

In this work, we report the first (to our knowledge) direct measurement of a mechanically induced transition between the oxy and deoxy states of the Hb in an RBC. With the use of two optical traps, the RBC was held and stretched while the Raman spectrum was excited with an additional beam. Changes in known oxygenation marker bands showed a transition to a deoxy state when an oxy RBC was stretched. We propose that the transition is due to an applied strain to the Hb molecules, which is a result of enhanced Hb neighbor-neighbor and Hb-membrane rates of interaction that occur upon cell stretching. The Hb neighbor-neighbor interaction was examined by modeling a simple two-Hb binding system and relating the effects of the resulting configuration to the oxygen affinity.

With this work, we present a robust optical system that provides a novel approach to studying isolated cells by using, simultaneously, optical tweezers force microscopy and chemical monitoring by Raman spectroscopy.

MATERIALS AND METHODS

Raman measurement

The multitrap Raman setup employed in this study has been described elsewhere and used successfully for Raman studies of living cells (26). Fig. 1 is a depiction of the setup used.

Briefly, a diode laser operating at 785 nm was used for the excitation of Raman spectra with an average power of ~5 mW at the sample. The cells were placed inside a custom-made sample holder with an 80-μm-thick coverslip. The holder was placed on an inverse Olympus IX 51 microscope equipped with a 100×1.3 NA oil immersion objective and a micrometer-controlled x-y stage. The backscattered light was collected by the microscope objective; it first passed through a holographic notch filter and then through a confocal system with a 100-μm pinhole. The spectrometer had a 600 lines/mm grating and was fitted with a thermoelectrically controlled
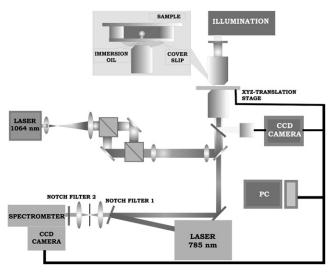

FIGURE 1 Schematic of the confocal Raman spectroscopy system with a dual-spot optical trap.

charge-coupled device (CCD), cooled to $-100°$C. A CCD camera attached to the microscope provided optical images during experiments. Raman spectra were recorded with a spectral resolution of 3 cm^{-1}.

A 1064 nm diode laser was used for the dual-spot trap. The expanded and collimated beam was directed through an interferometer before entering a second collimating lens system, which conjugates the image from the movable mirror planes to the back of the microscope objective. The movement of the mirrors in either arm of the interferometer will then result in x-y movement of the trap without changes in its intensity and shape, thus keeping the trapping potential of the traps the same. By allowing one of the collimating lenses in front of the interferometer to be movable, the trap beams can be slightly shifted axially such that they are in the same x-y plane as the Raman excitation beam. The beams were passed through the same microscope objective with an average power of ~10 mW at the sample.

For the measurement, we held the cell with the dual-spot trap and aligned it such that the Raman beam passed through its center. Raman spectra were then recorded for the cell in its equilibrium and stretched positions. We define the equilibrium position as the point where both beams trap the cell such that it is hindered from rotation while being minimally constrained in the stretch direction. The traps are positioned to keep the cell as close to its free length as possible to achieve this. For the stretched position, the cell was stretched to the maximum extent possible with the given power of the 1064 nm traps. At this power, the force applied to the cell, which is in the range of tens of pico-Newtons, is suitable for RBC stretching without irreversible damage (19,20). The in vivo aspects of this measurement are demonstrated by the fact that no dielectric beads are used to attach to the cell, and the power and acquisition times fall well under the limits for cell heating and photodegradation (4).

Sample preparation

Human serum albumin (HSA) and phosphate buffered saline (PBS, pH = 7.4) were obtained from Sigma-Aldrich (Madrid, Spain). The aqueous solutions were prepared by using deionized water. For the Raman measurements, blood obtained by venipuncture from healthy volunteers was diluted 1:100 with a mixture of HSA (2 mg/mL) and PBS. All Raman spectra were recorded immediately after blood was taken and diluted in the media solution. To demonstrate the in vivo aspects and Raman sensitivity of the system, the oxygenation of the RBCs was not done chemically. Although this increased the necessary cell sample size, the data show that consistent results were still obtained for oxy RBCs found in the blood sample.

Protein binding modeling

The Protein Data Bank x-ray crystallographic structure 1HHO (27) was the starting point for the computational investigations. This structure corresponds to the oxy R species. Two 1HHO tetramers were rigidly docked using the FT-dock (28) and pyDock (29) programs. FT-dock is a geometric recognition search engine for rigid-body proteins that is based on the Fourier correlation algorithm of Katchalski-Katzir et al. (30). The protein-protein poses produced by FT-dock were scored, i.e., energetically ranked, using py-Dock. The pyDock scoring system uses Coulombic electrostatics, a distance-dependent dielectric, and an implicit desolvation energy term that uses special atomic solvation parameters, and has been successful in scoring rigid-body docking sets (29).

RESULTS

Images of the RBC in the equilibrium and stretched states are shown in Fig. 2. The elongated RBC reflects the maximum stretching that could be achieved, which is approximated from the image to be ~40% of the original size. Fig. 3 is a sample raw Raman spectrum with the cell trapped in its equilibrium position. The large background due to the water
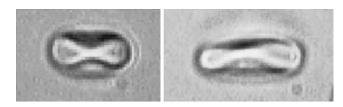
FIGURE 2   Camera image of the RBC trapped by two beams in the equilibrium (*left*) and stretched (*right*) conditions.

and media, along with the low signal/noise ratio due to the low Raman scattering cross section of the cell, necessitates background removal and smoothing. A five-point adjacent averaging smoothing was applied, followed by subtraction of the Raman spectra of the media alone. The resulting spectra, given in Fig. 4 for both the equilibrium and stretched conditions, are divided into the three well-characterized regions of the Hb (14,31). Many of the peaks align well between the two states, except for the small regions that are highlighted in gray. Fig. 5 contains the expansions of these ranges to clearly visualize the changes. The highlighted bands were isolated and the curved background was removed to obtain a fair comparison of frequency position and intensity. The background removal technique is based on a simple geometric algorithm and is unique in that a fit is not required (32). It was previously employed to study low Raman signals (33). To further verify the absence of spurious peaks due to the data processing, multiple Raman spectra of the media of RBC samples were measured and put through the same smoothing and background removal (using a control measurement of the media alone) procedure. In all instances, only a flat line resulted at the noise level.

For the success rate statistic, only cells that initially gave oxy Raman peaks were considered. In the experiment, 25 cells satisfied that criterion, and 14 of those cells gave results that were completely consistent with Figs. 4 and 5 after being stretched. The rest of the cell sample yielded a mixed consistency without complete agreement between all of the frequency regions in the Raman spectra. There are a number of reasons for this, including variances from cell to cell in ox-
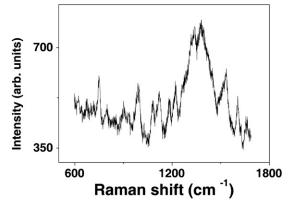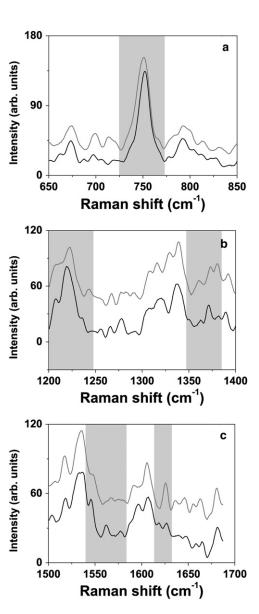

FIGURE 4   Raman spectra of equilibrium (*top spectra*) and stretched (*bottom spectra*) states of the RBC after smoothing and background subtraction. The spectra are separated into three well-characterized regions. The shaded areas represent the bands that changed consistently between equilibrium and stretched conditions for the majority of the sample of cells.

ygenation levels, elasticity, and the amount of Hb in the excitation volume before and after stretching. The acquisition time was 30 s for each spectrum. To test for possible photodegradation effects, Raman spectra were recorded for RBCs held in the dual-spot trap before and after a time period of 2 min. Minimal to no changes were seen in the spectra.

DISCUSSION

Changes in Raman spectra due to stretching

A strong band at 750 cm^{-1} (Fig. 5 *a*) was measured from the RBCs, which came from the C-N-C breathing stretch

FIGURE 3   Sample raw Raman spectrum of an RBC trapped with two beams in its equilibrium position.
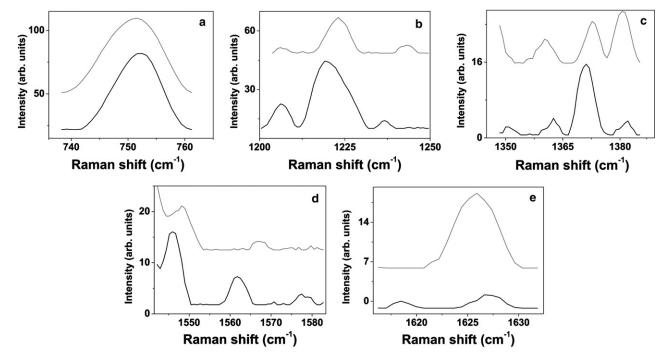
FIGURE 5 Close-up views of the highlighted bands from Fig. 4. For each graph, the top and bottom spectra are from the equilibrium and stretched states, respectively.

vibration in the porphyrin ring. When the RBC was stretched, we observed that this peak shifted up slightly in frequency and its linewidth became narrower. The amount of shifting and narrowing varied from cell to cell; however, the direction (an upward shift in frequency and a decrease in linewidth) was consistent. In the sample spectrum shown here, there is an increase of 3 cm^{-1} (750 cm^{-1} to 753 cm^{-1}) for the peak position and a decrease of 9 cm^{-1} (23–14 cm^{-1}) for the linewidth. Both shifts are close to the median values for the cell group. Peak positions and linewidths were determined by fitting the curves to a Voigt profile and extracting the Lorentzian component. A frequency shift of this peak was observed previously in a study comparing the Raman spectra of healthy and sick blood cells (15). In that study, the frequency increase observed was attributed to closer packing of the porphyrin structures in the infected cells, which would lead to a ''stronger'' vibrational mode. In our case, the stretching of the RBC could place a strain on the Hb structures that alters the breathing mode by changing its frequency or by dampening out-of-plane vibrations and other modes that add disorder, thus reducing the broadening effects in this Raman band.

The important trend noted in this study is that when we observed the narrowing of this band, consistent changes were seen in the regions that contain bands that are known to be affected by the state of oxygenation of the Hb. The most striking effect is observed in the band at 1625 cm^{-1} (Fig. 5 e), assigned to the C-C vibration of the polyporphyrin side chain, which disappears upon stretching. This disappearance was observed in previous studies that compared

Raman bands between oxy and deoxy RBCs (14–17,34). Upon dissociation of oxygen, the planar structure deforms out of plane (termed porphyrin doming), consequently causing this band to disappear. A complete disappearance was not seen here, most probably due to the mixed oxygenation states of each heme in the cell; however, the sharp decrease that occurs after stretching indicates a strong transition toward deoxygenation.

We also observe changes in other regions that are indicative of the oxygenation and spin state of the center iron atom. Bands appearing around 1500 cm^{-1} are assigned as spin-state markers (14,16,17,34) because these vibrations are from C-C bonds in the ring that are affected by the spin state of the iron atom. From Fig. 5 d, we measure a small band at 1567 cm^{-1} and a shoulder peak at 1548 cm^{-1} in the equilibrium state of the RBC. The former is typical of low-spin ferrous iron (Fe^{2+}), which is a characteristic of bound oxygen. For the deoxy state, the iron is most likely in a high spin state, and in this condition the Raman band should split to a lower and a higher band, which also is observed here at 1546 cm^{-1} and 1578 cm^{-1} in the stretched state. All three values agree with previous studies of oxy, deoxy, and varying iron oxidation states of Hb (14,17). We also observe that the center low spin peak reappears as a stronger band positioned at a slightly lower frequency in the stretched state. This is most likely due to the presence of Hb structures that have not changed completely to the deoxy condition, or to an alteration of the vibration due to the external strain.

The 1200–1300 cm^{-1} region contains the in-plane bending vibrations of the methine C-H (16). These bonds are

affected by the coordination between the iron atom and the porphyrin ring. The measured bands for this region are given in Fig. 5 b. We measure peaks at 1243 cm^{-1} and 1222 cm^{-1} in the equilibrium that shift to 1236 cm^{-1} and 1218 cm^{-1} after stretching. A third peak is observed in both conditions at 1206 cm^{-1}, with a higher intensity measured in the stretched state. The decrease in frequency of these bands between the equilibrium and stretched states agrees with previous observations of these bands between oxy and deoxy RBCs (14,16,17). The change is due to the decrease in strength of the coordination between iron and the porphyrin ring as the atom is pushed out from the center during the oxy-to-deoxy transition.

The 1350–1400 cm^{-1} region contains bands that come from C-N stretching in the heterocyclic ring that surrounds the iron atom. The frequencies of the band are affected by the oxidation state of Fe because of the electron back donation from the Fe that weakens the bond. Thus, this region contains the "oxygenation state marker" of the heme (15,16); however, this dependence has been questioned (14,35,36). A band around 1350 cm^{-1} has typically indicated the ferrous (Fe^{2+}) state of iron, and with bound oxygen the shift to a ferric-like (Fe^{3+}) state gives a band around 1370 cm^{-1} (16,17). However, a number of studies have produced mixed results for this region. In some, both bands have appeared in the oxy and deoxy Hb due to the higher electron back donation of Fe^{2+}, which either weakens the C-N stretch mode, causing a lower Raman frequency, or increases the mode because the lower electron density around the iron atom causes it to act more ferric (15). In other studies, this band was simply invariant to oxygenation (14,35). Here, we find three peaks in the 1360–1380 cm^{-1} region for the equilibrium state (Fig. 5 c). In the stretched condition, the lower and higher bands drop in intensity, and the middle peak close to 1370 cm^{-1} remains. A smaller peak at 1350 cm^{-1} also appears. Thus, we find evidence of oxy markers in the equilibrium condition that seem to change to deoxy, based on either the decreased intensities or the appearance of the band at the lowest frequency in this region in the stretched condition.

Overall, we observed strong evidence of a transition from oxy to deoxy Hb when an RBC is stretched. The measured Raman bands for the equilibrium and stretched conditions of the cell agree with those previously measured in oxy and deoxy states, respectively. Many of the oxygenation or spin state markers are based on the position of the iron atom relative to the porphyrin ring and the resulting deformation of this ring. Thus, an external strain applied to the Hb can account for these band changes.

Mechanisms for mechanically induced change in oxidation

One cause of this change could be related to the membrane becoming more permeable due to the stretching. However, earlier studies have questioned the significance of the membrane in affecting oxygen diffusion altogether (37,38). A second explanation could be based on pressure effects. An early study observed no shift in the oxygenation equilibrium of bovine Hb when the pressure was increased from 1 to 680 atm (39). This early experimental procedure was brought into question in a recent study that measured the apparent specific volumes of human deoxy and oxy Hb (40). However, the change in volume reported was a minimal increase of only 0.2% when going from T to R. Another work showed that the Raman spectrum of oxy Hb changed under even higher pressure (GPa range); however, the altered spectrum differed from deoxy Hb, which led to the conclusion that the dissociation was thermally induced (41). Considering our experimental conditions, the creation of such high pressures, which seems necessary to alter the Hb protein either thermally or by changing its specific volume, is not possible in the RBC during stretching. Thus, there must exist a more prevalent mechanism for the change in oxygenation observed in our data.

The stretching of the RBC affects the Hb in two ways that promote both the release of oxygen and the transition from the oxy (R) to the deoxy (T) condition. First, stretching in this manner causes the elongation of the cell to a more ellipsoidal form, which increases the area/volume ratio (due to the membrane folding) and the area of contact of the membrane with the cytosol (19). Previous studies have established the roles of the membrane in regulating RBC oxygen transport and glucose metabolism (42,43). The former is the main cycle of the O_2-CO_2 exchange, where the band 3 macrocomplex in the membrane accepts carbon dioxide and transforms it into a release of protons in the vicinity of the membrane-cytoplasm interface. Thus, the oxygen release, a result of the acidification of the local area, occurs most rapidly for oxy Hbs that are in this region. A secondary role that enhances this effect is the glucose regulation due to binding of deoxy Hb to the cytoplasmic side of band 3 (43). The deoxy Hb has a higher affinity to this binding than the oxy Hb and competes with glycolytic enzymes for this site (43,44). The enzyme inhibition results in the increase of glucose flux, which leads to the production of ATP and organic phosphates, and the latter further promotes oxygen release from free Hbs. The Hb-membrane interaction occurs, quite obviously, close to the membrane, and thus an increase in the area of contact between the cytoplasm and membrane would lead to enhancement of the oxygenation transition.

The second effect of stretching is an increased rate of interaction between neighboring Hbs. Elongating the RBC can lead to a decrease in the internal volume due to the outflux of water and solutes when the cell is under stress (45). The result is an increase in Hb concentration, which promotes the neighbor-neighbor interaction of Hbs. The interaction could inhibit movement of the protein, which would affect the oxidation state because the oxidation/deoxidation of the Hb is an interplay between chemical bonding and

physical conformational changes of the structure. The construction and orientation of the heme group are such that a small displacement of the iron atom will be amplified throughout the rest of the subunits. Following the model of Perutz (1,46), when an oxygen atom binds to the iron center of the porphyrin ring of a heme group, the iron atom is pulled in to the ring center. This leads to a large movement of the proximal histidine relative to the ring. The histidine movement causes changes in the structures, with the most notable being the movement of the F-helix toward the heme group. This movement induces other conformational changes that finally break the salt bridges that hold the Hb in its deoxy form. With the salt bridges removed, the oxygen affinity is raised because the subunits are no longer constrained, thus demonstrating the cooperative aspect of oxygen binding in Hb. Such a mechanism was proposed upon inspection of the oxy and deoxy crystallographic structures (1). Recently, this interplay between conformational changes and binding affinities was quantified by means of theoretical modeling using mixed quantum mechanics and molecular mechanics techniques (47). It was shown that the residues involved in the quaternary contacts are responsible for the differential in affinity. In particular, the largest contributions are assigned to the anchor points around the F-helix. The conformational quaternary changes introduce constraints to the F-helix in the T structure and hinder the necessary iron motion, reducing the oxygen affinity.

The nonbonded interaction of neighboring Hbs could apply a similar constraint to the structural reorganization of the protein. At the time of this work, no experimental or theoretical study of this effect had been conducted (to our knowledge), so we studied the limit of this mostly electro-static interaction by modeling the binding of two Hb molecules. Using the protein-protein docking algorithms described in Materials and Methods, we searched for the most probable interaction between different units. Three of the first four complexes involved large contacts in the F-helix. The lowest energy configuration found is depicted in Fig. 6. As can be seen in Fig. 6 b, the favorable configuration results in strong contacts at the F-helix (indicated by arrows), potentially hindering its movement. Thus, we may be observing the imposition of constraints limiting the F-helix rearrangement that are induced (initially) not by quaternary contacts, as previously seen in the single protein unit, but by neighbor-neighbor interactions. These interactions may even lock a low-oxygen-affinity or deoxy Hb into an oxy-like R structure, which gives another explanation for the invariance of some Raman bands that are associated with oxygenation changes.

The strong relation between mechanical forces and chemical changes in the Hb structure leads to the question of reversibility of the process. The connection of force and oxygenation should be reversible in terms of general physiology of the cell and the thermodynamics of the Hb. For the former, there is a constant exchange of oxygen and carbon dioxide in the RBC that causes the Hb to go back and forth between its two structures as the cell ages. The cell deforms in the respiratory area as well, and thus a heightened interaction with the membrane would make a deoxy Hb more available to free oxygen. For the latter, a force could be applied to the Hb that would balance the strain in the T structure of the deoxy, pushing the heme groups further out from the protein to receive oxygen. The idea that this force could come from neighbor-neighbor interactions of the Hb is
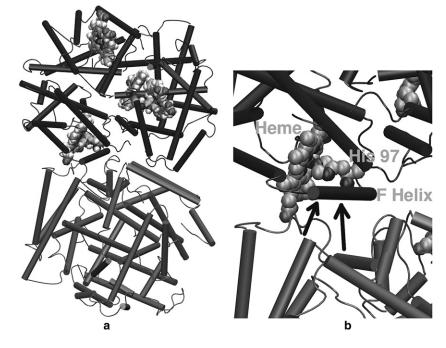

FIGURE 6 Global representation (*a*) and close-up view (*b*) of the lowest energy configuration of the binding of two Hb molecules modeled from the protein-protein docking algorithms. The arrows identify the points of contact at the F-helix.

questionable because of the consistent binding at the F-helix. In our experiments, without changing the conditions of the cell surroundings, an effect was observed in the reverse direction; however, it was not present at nearly as consistent a rate as the results presented here. One issue is that the oxygen content of the media in the ambient air is not high enough to promote the influx of O_2. To better analyze this, the cell media should be saturated with oxygen to reverse the gradient across the membrane, which is a future consideration for this work.

Overall, the results fit well with the structure and function of the RBC and Hb. The effect is realistic when one considers the mechanochemical character of the Hb protein and the physiological aspects of the RBC in terms of its unique deformability as it travels through vessels and capillaries. Indeed, most proteins could act as mechanochemical transducers because many aspects of chemical binding and enzymatic processes involve changes in protein structure dimensions.

CONCLUSIONS

We have presented Raman spectra of equilibrium and stretched RBCs, and discussed the spectral changes based on mechanically induced effects. By comparing the Raman spectra of equilibrium and stretched RBCs with results from previous studies of oxy and deoxy RBCs, we conclude that cells with a significant oxygen concentration were pushed to a deoxy state when stretched with optical tweezers. The mechanically induced change in oxygenation state is based on the enhanced rates of interaction between neighboring Hbs, and Hb and the membrane, which is a consequence of stretching the cell. The Hb neighbor interaction is further studied by modeling the binding of two Hb proteins. The results of the model show that the Hb components responsible for its oxy state become constrained. The overall result reveals a bidirectional relationship between chemical binding and mechanical force in the oxygenation cycle of the Hb structure.

REFERENCES

1. Perutz, M., A. Wilkinson, M. Paoli, and G. Dodson. 1998. The stereo-chemical mechanism of the cooperative effects in hemoglobin revisted. *Annu. Rev. Biophys. Biomol. Struct.* 27:1–34.

2. Khan, S., and M. Sheetz. 1997. Force effects on biochemical kinetics. *Annu. Rev. Biochem.* 66:785–805.

3. Ashkin, A., D. Dziedzic, and T. Yamane. 1987. Optical trapping and manipulation of single cells using infrared laser beams. *Nature.* 330:769–772.

4. Svoboda, K., and S. Block. 1994. Biological applications of optical forces. *Annu. Rev. Biophys. Biomol. Struct.* 23:247–285.

5. Grier, D. 2003. A revolution in optical manipulation. *Nature.* 424:810–816.

6. MacDonald, M., G. Spalding, and K. Dholakia. 2003. Microfluidic sorting in an optical lattice. *Nature.* 426:421–424.

7. Petrov, D. 2007. Raman spectroscopy of optically trapped particles. *J. Opt. A: Pure Appl. Opt.* 9:s139–s153.

8. Xie, C., M. Dinno, and Y. Li. 2002. Near-infrared Raman spectroscopy of single optically trapped biological cells. *Opt. Lett.* 27:249–251.

9. Deng, J., Q. Wei, M. Zhang, Y. Z. Wang, and Y. Li. 2005. Study of the effect of alcohol on single human red blood cells using near-infrared laser tweezers Raman spectroscopy. *J. Raman Spectrosc.* 36:257–261.

10. Chan, J., D. Taylor, S. Lane, T. Zwerdling, J. Tuscano, et al. 2005. Nondestructive identification of individual leukemia cells by laser trapping Raman spectroscopy. *Anal. Chem.* 80:2180–2187.

11. Creely, C., G. Volpe, G. Singh, M. Soler, and D. Petrov. 2005. Raman imaging of floating cells. *Opt. Express.* 12:6105–6110.

12. Liu, Y., D. Cheng, G. Sonek, M. Berns, C. Chapman, et al. 1995. Evidence of localized cell heating induced by infrared optical tweezers. *Biophys. J.* 68:2137–2144.

13. Singh, G., G. Volpe, C. Creely, H. Grötsch, I. Geli, et al. 2006. The lag phase and G_1 phase of a single yeast cell monitored by Raman microspectroscopy. *J. Raman Spectrosc.* 37:858–864.

14. Wood, B., B. Tait, and D. McNaughton. 2001. Micro-Raman characterisation of the R to T state transition of haemoglobin within a single living erythrocyte. *Biochim. Biophys. Acta.* 1539:58–70.

15. Ong, C., Z. Shen, K. Ang, U. Kara, and S. Tang. 1999. Resonance Raman microspectroscopy of normal erythrocites and Plasmodium berghei-infected erythrocites. *Appl. Spectrosc.* 53:1097–1101.

16. Brunner, H., A. Mayer, and H. Sussner. 1972. Resonance Raman scattering on the haem group of oxy- and deoxyhaemoglobin. *J. Mol. Biol.* 70:153–156.

17. Venkatesh, B., S. Ramasamy, M. Mylrajan, R. Asokan, P. Manoharan, et al. 1999. Fourier transform Raman approach to structural correlation in hemoglobin derivatives. *Spectrochim. Acta [A].* 55: 1691–1697.

18. Singer, W., M. Frick, T. Haller, S. Bernet, M. Ritsch-Marte, et al. 2003. Mechanical forces impeding exocytotic surfactant release revealed by optical tweezers. *Biophys. J.* 84:1344–1351.

19. Dao, M., C. Lim, and S. Suresh. 2003. Mechanics of the human red blood cell deformed by optical tweezers. *J. Mech. Phys. Solids.* 51:2259–2280.

20. Sleep, J., D. Wilson, R. Simmons, and W. Gratzer. 1999. Elasticity of the red cell membrane and its relation to hemolytic disorders: an optical tweezers study. *Biophys. J.* 77:3085–3095.

21. Lenormand, G., S. Hénon, A. Richert, J. Siméon, and F. Gallet. 2001. Direct measurement of the area expansion and shear moduli of the human red blood cell membrane skeleton. *Biophys. J.* 81:43–56.

22. Guck, J., R. Ananthakrishnan, T. Moon, C. Cunningham, and J. Käs. 2000. Optical deformability of soft biological dielectrics. *Phys. Rev. Lett.* 84:5451–5454.

23. Li, C., and K. Liu. 2008. Nanomechanical characterization of red blood cells using optical tweezers. *J. Mater. Sci. Mater. Med.* 19: 1529–1535.

24. De Luca, A., G. Rusciano, R. Ciancia, V. Martinelli, G. Pesce, et al. 2008. Spectroscopical and mechanical characterization of normal and thalassemic red blood cells by Raman tweezers. *Opt. Express.* 16:7943–7957.

25. Vera, C., R. Skelton, F. Bossens, and L. Sung. 2005. 3-D nanomechanics of an erythrocyte junctional complex in equibiaxial and anisotropic deformations. *Ann. Biomed. Eng.* 33:1387–1404.

26. Creely, C., G. Singh, and D. Petrov. 2005. Dual-wavelength optical tweezers for confocal Raman spectroscopy. *Opt. Commun.* 245:465–470.

27. Shaanan, B. 1983. Structure of human oxyhaemoglobin at 2.1 Å resolution. *J. Mol. Biol.* 171:31–59.

28. Gabb, H., R. Jackson, and M. Sternberg. 1997. Modelling protein docking using shape complementarity, electrostatics and biochemical information. *J. Mol. Biol.* 272:106–120.

29. Cheng, T., T. Blundell, and J. Fernandez-Recio. 2007. pyDock: electrostatics and desolvation for effective scoring of rigid-body protein-protein docking. *Proteins.* 68:503–515.

30. Katchalski-Katzir, E., I. Shariv, M. Eisenstein, A. Friesem, C. Aflalo, et al. 1992. Molecular surface recognition: determination of geometric

fit between proteins and their ligands by correlation techniques. *Proc. Natl. Acad. Sci. USA*. 89:2195–2199.

31. Hu, S., K. Smith, and T. Spiro. 1996. Assignment of protoheme resonance Raman spectrum by heme labeling in myoglobin. *J. Am. Chem. Soc*. 118:12638–12646.

32. Mikhailyuk, I., and A. Razzhivin. 2003. Background subtraction in experimental data arrays illustrated by the example of Raman spectra and fluorescent gel electrophoresis patterns. *Instrum. Exp. Tech*. 46:765–769.

33. Rao, S., K. Mantey, J. Therrien, A. Smith, and M. Nayfeh. 2007. Molecular behavior in the vibronic and excitonic properties of hydrogenated silicon nanoparticles. *Phys. Rev. B*. 76:155316–155319.

34. Spiro, T., J. Stong, and P. Stein. 1979. Porphyrin core expansion and doming in heme proteins. New evidence from resonance Raman spectra of six-coordinate high-spin iron(III) hemes. *J. Am. Chem. Soc*. 101:2648–2655.

35. Spaulding, L., C. Chang, N. Yu, and R. Felton. 1975. Resonance Raman spectra of metallooctaethylporphyrins. Structural probe of metal displacement. *J. Am. Chem. Soc*. 97:2517–2525.

36. Szabo, A., and L. Barron. 1975. Resonance Raman studies of nitric oxide hemoglobin. *J. Am. Chem. Soc*. 97:660–662.

37. Kreuzer, F., and W. Yahr. 1960. Influence of red cell membrane on diffusion of oxygen. *J. Appl. Physiol*. 15:1117–1122.

38. Subczynski, W., L. Hopwood, and J. Hyde. 1992. Is the mammalian cell plasma membrane a barrier to oxygen transport? *J. Gen. Physiol*. 100:69–87.

39. Johnson, F., and F. Schlegel. 1948. Hemoglobin oxygenation in relation to hydrostatic pressure. *J. Cell. Comp. Physiol*. 31:421–425.

40. DeMoll, E., D. Cox, E. Daniel, and A. Riggs. 2007. Apparent specific volume of human hemoglobin: effect of ligand state and contribution of heme. *Anal. Biochem*. 363:196–203.

41. Alden, R., J. Satterlee, J. Mintorovitch, I. Constantinidis, M. Ondrias, et al. 1989. The effects of high pressure upon ligated and deoxyhemoglobins and myoglobin. *J. Biol. Chem*. 264:1933–1940.

42. De Rosa, M., C. Alinovi, A. Galtieri, A. Russo, and B. Giardina. 2008. Allosteric properties of hemoglobin and the plasma membrane of the erythrocyte: new insights in gas transport and metabolic modulation. *IUBMB Life*. 60:87–93.

43. Messana, I., M. Orlando, L. Cassiano, L. Pennacchietti, C. Zuppi, et al. 1996. Human erythrocyte metabolism is modulated by the O_2-linked transition of hemoglobin. *FEBS Lett*. 390:25–28.

44. Walder, J., R. Chatterjee, T. Steck, P. Low, G. Musso, et al. 1984. The interaction of hemoglobin with the cytoplasmic domain of band 3 of the human erythrocyte membrane. *J. Mol. Biol*. 259:10238–10246.

45. Jay, A., and P. Canham. 1977. Viscoelastic properties of the human red blood cell membrane II. Area and volume of individual red cells entering a micropipette. *Biophys. J*. 17:169–170.

46. Perutz, M. 1970. Stereochemistry of cooperative effects in hemoglobin. *Nature*. 228:726–734.

47. Alcantara, R., C. Xu, T. Spiro, and V. Guallar. 2007. A quantum-chemical picture of hemoglobin affinity. *Proc. Natl. Acad. Sci. USA*. 104:18451–18455.